

Improved Algorithm for Direct Mean Torque Control of an Induction Motor

Erich Flach

Department of Power Electronics and Drives

Darmstadt University of Technology

Landgraf-Georg-Str. 4

D-64283 Darmstadt

ABSTRACT

An improved algorithm of Direct Mean Torque Control (DMTC) of an induction motor is presented. DMTC combines the good dynamic performance of Direct Torque Control (DTC) with the advantages of time equidistant control algorithms for digital implementation in signal processor based systems. The predictive algorithm allows even to exploit machines with extremely small leakage inductance.

At low speed, the new flux controller allows to decrease the torque ripple. At high speed, a new algorithm to calculate the on-time of voltage vectors shows a better switching behaviour and even less torque ripple, whereas the dynamical performance is kept. The basic idea is to estimate the inevitable torque ripple in steady state and match it at the end of the cycle. Thus, the mean torque is directly controlled as well. The criteria how to choose the appropriate vector depend on the state of the machine and the deviations of flux and torque. The algorithms are well suited for an implementation on digital signal processor based systems with less external hardware requirement. Simulations and experimental results confirm the validity of the control scheme.

INTRODUCTION

Classical field orientation has achieved a good performance in many applications where a converter with high switching frequency is used. In this case, a micro-controller may satisfy the needs of calculation power. Direct methods achieve a higher dynamic performance

since they do not use a modulator, i. e. PWM. Using comparators with hysteresis, analog devices are commonly used to realize DTC [1], or similar methods. If one has to keep the torque in a preset hysteresis-band with a minimum of switching events, [2] is best suited, but current harmonics are rather large. In modern drives, a digital implementation offers more flexibility, and it is easier to bring it into service. A quasi-analog realization has been presented by [3]. The sampling frequency must be significantly higher than the desired switching frequency to keep the torque in the hysteresis band. A prediction of the switching events similarly to [4] is possible, but the sampling events are no longer equidistant. Just using a constant cycle time is advantageous for digital implementation. So the predicted time may be fixed. For a given time interval, it is possible to forecast several switching events in order to distribute the computation time over the cycle. A first approach has been presented in [5]. Since the influence of the zero vector was not taken into account to estimate the on-time of the voltage vectors, an adaptation algorithm was necessary to compensate the torque offset. Another approach to DTC with constant cycle time is Direct Mean Torque Control (DMTC) [6]. This paper presents an improved method of DMTC that provides less torque ripple at lower speed. This is achieved by a more sophisticated treatment of the mainly flux increasing vectors, which may increase or even decrease the torque. At higher speed, DMTC [6] may cause some suspicious switching behaviour due to the equation used to calculate the on-time of the voltage vector. The new method calculates the on-time in a way that steady state of torque is directly reached at the end of the cycle.

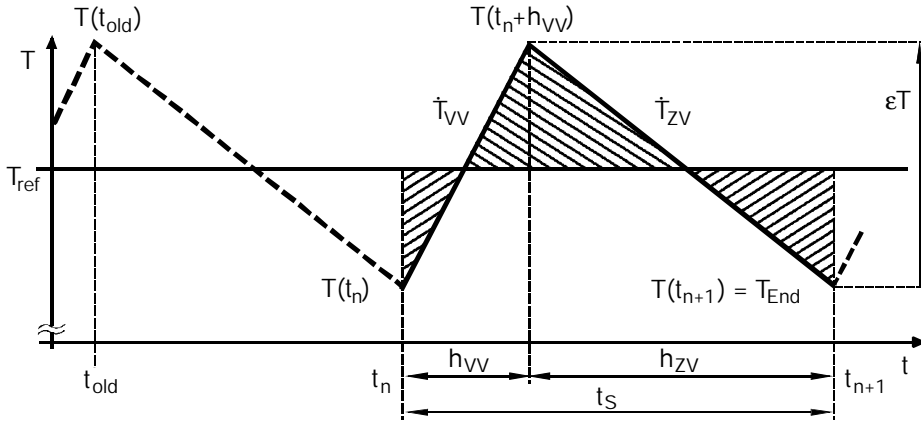


Fig. 3: Typical operation cycle of DMTC

The positive direction, thus VVm+1,2,3, is chosen if:

$$\Delta T \geq \dot{T}_{ZV} \cdot t_s + \frac{1}{2} \cdot \epsilon T \quad (4)$$

with $\Delta T = T_{ref} - T(t_n)$. Otherwise, we use VVm-0,1,2. Since VVm±1 is normally the most taken VV, we assume ϵT as the "virtual hysteresis width" while using VVm±1. ϵT can be expressed as:

$$\epsilon T = \dot{T}_{VV} \cdot h_{VV} = -\dot{T}_{ZV} \cdot h_{ZV} = -\dot{T}_{ZV} \cdot (t_s - h_{VV}) \quad (5)$$

\dot{T}_{VV} can be calculated by deriving eq. 3. Since the state of the machine at t_n+h_{VV} is not known yet, it is the easiest way to get \dot{T}_{ZV} from the last cycle:

$$\dot{T}_{ZV} \cong \frac{T(t_n) - T(t_{old})}{t_n - t_{old}} \quad (6)$$

We eliminate h_{VV} in eq. 5 to get:

$$\epsilon T = -\frac{\dot{T}_{VV} \cdot \dot{T}_{ZV}}{\dot{T}_{VV} - \dot{T}_{ZV}} \cdot t_s \quad (7)$$

With $\dot{T}_{VV} = \dot{T}_{VV1}$, this equation is used in eq. 1 to determine the instantaneous torque to be reached at the end of the cycle. To avoid torque offsets, ϵT must be limited to $\epsilon T \geq \dot{T}_{VV1} \cdot h_{min}$.

Torque Control

For given $\dot{T}_{VV} = \dot{T}_{VV0,1,2}$ of VVm±0,1,2, we search its on-time h_{VV} to attain exactly T_{End} . The torque $T(t_{n+1})$ at the end of the cycle can be expressed as:

$$T(t_{n+1}) = T(t_n) + \dot{T}_{VV} \cdot h_{VV} + \dot{T}_{ZV} \cdot (t_s - h_{VV}) \quad (8)$$

Solving this equation for h_{VV} leads finally to:

$$h_{VV} = \frac{T_{ref} - T(t_n) - \frac{1}{2} \cdot \epsilon T - t_s \cdot \dot{T}_{ZV}}{\dot{T}_{VV} - \dot{T}_{ZV}} \quad (9)$$

Ordinarily, a VV should only be applied, if the result of eq. 9 is within $h_{min} \leq h_{VV} \leq t_s - h_{min}$. In this case, the torque will stay in the "virtual hysteresis band". Since ϵT has been calculated for \dot{T}_{VV1} , VVm±1 ($\Rightarrow h_{VV1}$) satisfies the demand. For lower angular speed of the flux vector, VVm±2 is well suited, too, whereas VVm±0 has to be checked out.

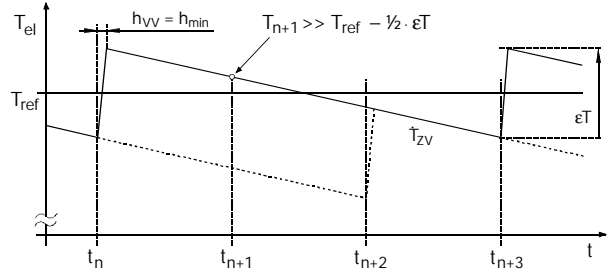


Figure 4: Peculiarity of novel method for $\epsilon T \cong \dot{T}_{ZV} \cdot t_s$

A special problem crops up if $\epsilon T \geq \dot{T}_{ZV} \cdot t_s$, illustrated in fig. 4. To command the torque as close as possible at T_{ref} , it is favourable to switch the VV at t_n , although $T(t_{n+1})$ would be pretty far from the aspired value $T_{ref} - \frac{1}{2} \cdot \epsilon T$. By the way, it's obvious to notice that the switching frequency drops down. Calculating the on-time h_{VV} according to eq. 9 leads to $h_{VV} < \frac{1}{2} \cdot h_{min}$, rounded towards zero. The torque would follow the dotted line in fig. 4. It falls below the estimated band limit and a negative torque offset would be observed. Therefore, if eq. 9 leads to on-times $h_{VV} < h_{min}$, we recalculate h_{VV} with the equation used in [4]. This often yields to on-times $h_{VV}(t_n) > \frac{1}{2} \cdot h_{min}$, rounded to h_{min} , thus tracking the continuous line in fig. 4. The principle is to equalize the differently hatched areas in fig. 3. We just recite the basic equations. We define the mean values

$$\bar{T}_{VV} = \frac{1}{2} \cdot (T(t_n) + T(t_n+h_{VV})) \quad (10a)$$

$$\bar{T}_{ZV} = \frac{1}{2} \cdot (T(t_n+h_{VV}) + T(t_{n+1})) \quad (10b)$$

$$\bar{T}_s = (\bar{T}_{VV} \cdot h_{VV} + \bar{T}_{ZV} \cdot h_{ZV}) / t_s \quad (10c)$$

Setting the mean value over the cycle $\bar{T}_s = T_{ref}$ leads to:

$$h_{VV} = t_s - \underbrace{\sqrt{t_s^2 - \frac{2 \cdot (T(t_n) - T_{ref}) \cdot t_s + \dot{T}_{ZV} \cdot t_s^2}{\dot{T}_{ZV} - \dot{T}_{NV}}}}_{= h_{ZV}} \quad (11)$$

Flux Control

Since high dynamic torque control is our main goal, the flux controller should not interfere with it. Similar to [1], [4], the stator flux is kept as close as possible on a circular trajectory. After the preselection of the $VVm\pm 0,1,2$, the flux controller uses the flux propagation and some supplementary rules to choose the appropriate VV. The length of the flux vector is given by

$$\Psi_{s,VV} = \left| \underline{\Psi}_{s,VV} \right| = \sqrt{\Psi_{sa}^2 + \Psi_{sb}^2} \quad (12)$$

Its derivative is

$$\dot{\Psi}_s = (\dot{\Psi}_{sa} \cdot \Psi_{sa} + \dot{\Psi}_{sb} \cdot \Psi_{sb}) / \Psi_s \quad (13)$$

For the VV, $\dot{\Psi}_{sa,b,VV}$ results from eq. 2, whereas for the ZV, $\dot{\Psi}_{s,ZV}$ itself can simply be taken from the last cycle similar to eq. 6:

$$\dot{\Psi}_{s,ZV} = (\Psi(t_{old}) - \Psi(t_n)) / (t_n - t_{old}) \quad (14)$$

Starting from eq. 9 resp. eq. 11 of the torque controller, and $\dot{\Psi}_s$, we can predict the evolution of the flux vector over the next cycle for each VV. At higher speed, the flux controller chooses between $VVm\pm 1$ and $VVm\pm 2$ to influence the flux. A common problem of DTC methods is the flux maintenance at lower speed, because the on-times of the VV decrease. First it is possible to check if the $VVm\pm 0$ is able to control either flux and torque as well. Its on-time h_{VV0} is limited to $h_{VV0,max}$ by the maximum flux increase which seems to be tolerable (using $\Delta\Psi$ from eq. 17a):

$$h_{VV0,max} = C_1 \cdot \frac{\Delta\Psi + C_2 \cdot \Psi_{ref}}{\dot{\Psi}_{VV0}} \quad (15)$$

Empirical tests showed acceptable results with $C_1 = 1.5$ and $C_2 = 2\%$. If eq. 9 leads to

$$h_{min} \leq h_{VV0} \leq h_{VV0,max} \quad (16)$$

Then $VVm\pm 0$ is adequate to control the torque. If this is not the case, and the flux cannot be preserved over several cycles, it is necessary to apply a flux-supporting VV (i. e. $VVm\pm 0$), although the torque control may be affected. If the flux-supporting VV is switched too late, flux decrease has become important, hence it requires a longer on-time. The idea in this paper is to detect the necessity of flux-supporting VV as soon as possible to diminish its influence over the torque. A basic intention was to find expressions which check out relationships between the influences of the switching states over the flux. Avoiding to compare with absolute quantities has the advantage of uncomplicated parameterization for different machines.

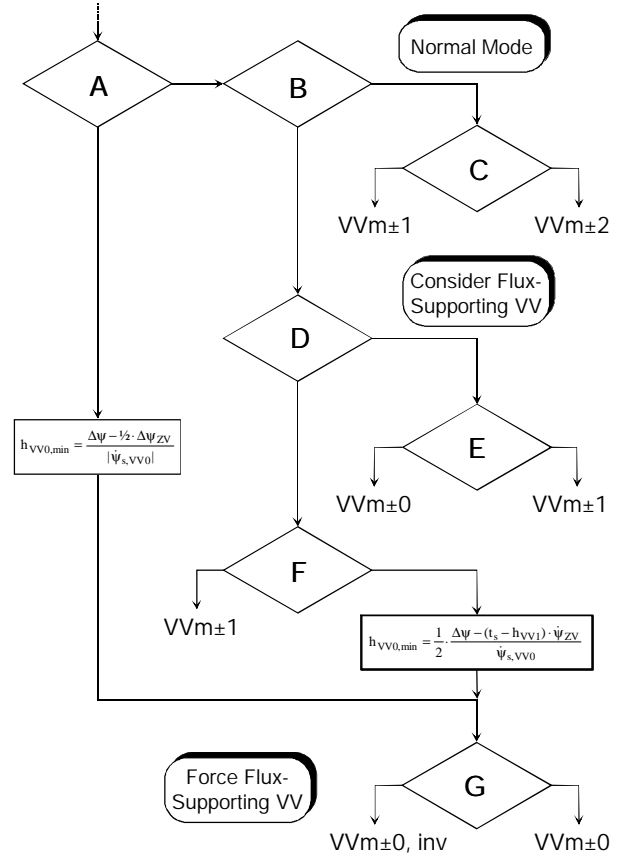


Figure 5: Flow chart of flux controller

The algorithm consists of a set of decision rules. We define its inputs as:

$$\Delta\Psi = \Delta\Psi(t_n) = \Psi_{ref}(t_n) - \Psi(t_n) \quad (17a)$$

$$\Delta\Psi_{VV0} = \Delta\Psi - 1/2 \cdot h_{VV0} \cdot \dot{\Psi}_{s,VV0} \quad (17b)$$

$$\Delta\Psi_{VV1} = \Delta\Psi - 1/2 \cdot h_{VV1} \cdot \dot{\Psi}_{s,VV1} \quad (17c)$$

$$\Delta\Psi_{VV2} = \Delta\Psi - h_{VV2} \cdot \dot{\Psi}_{s,VV2} - (t_s - h_{VV2}) \cdot \dot{\Psi}_{s,ZV} \quad (17d)$$

$$\Delta\Psi_{ZV} = \Psi(t_n) - \Psi(t_{old}) \quad (17e)$$

Fig. 5 shows the flow chart of the flux controller, which is performed in fig. 1, Block ⑥. There are three principle operation modes to enter:

- **“Normal Mode“** where to chose between flux increasing $VVm\pm 1$ or flux decreasing $VVm\pm 2$.
- **“Consider Flux-Supporting VV“** where $VVm\pm 0$ may only be switched without torque disruption, $VVm\pm 1$ otherwise.
- **“Force Flux-Supporting VV“** where $VVm\pm 0$ must be switched, although $T_{End,VV0} \neq T_{ref} - 1/2 \cdot \epsilon T$.

In „Flux-Supporting VV“ mode, if \dot{T}_{VV0} decreases the torque error (i. e. $\Delta T - \frac{1}{2} \cdot \varepsilon T$), $VVm\pm 0$ is switched for $h_{VV0,max}$ to keep the torque as good as possible. Otherwise, h_{VV0} is reduced and the switching order is inverted. This means, in order to minimize the torque error over the time, the ZV is applied first, thus preserved from the last cycle, and after it the VV. The resulting torque error over such a cycle can be taken into account by adding it to T_{ref} just for the next cycle.

The decision rules A-G in fig. 5 are mainly (\rightarrow condition is satisfied, \rightarrow otherwise):

- A:** $\Delta\psi \geq C_3 \cdot \psi_{ref}$ (i. e. $C_3 = 3\%$)
AND
 $\psi_s(t_n) - \psi_s(t_{n-1}) \leq 0$
 $\rightarrow G$ $\rightarrow B$
- B:** $\Delta\psi_{VV1} \leq 0$
 $\rightarrow C$ $\rightarrow D$
- C:** $|\Delta\psi_{VV1}| \leq |\Delta\psi_{VV2}|$
 $\rightarrow VVm\pm 1$ $\rightarrow VVm\pm 2$
- D:** $h_{min} \leq h_{VV0} \leq h_{VV0,max}$ (eq. 16)
 $\rightarrow E$ $\rightarrow F$
- E:** $|\Delta\psi_{VV0}| \leq |\Delta\psi_{VV1}|$
 $\rightarrow VVm\pm 0$ $\rightarrow VVm\pm 1$
- F:** $\Delta\psi > -0.75 \cdot t_s \cdot \dot{\psi}_{s,ZV}$
AND
 $h_{VV1} \cdot \dot{\psi}_{s,VV1} + (t_s - h_{VV1}) \cdot \dot{\psi}_{s,ZV} \leq 0$
 $\rightarrow G$ $\rightarrow VVm\pm 1$.
- G:** $sign(\dot{T}_{VV0}) = sign(\dot{T}_{VV1})$
 $\rightarrow VVm\pm 0$ first, then ZV, $h_{VV0}=h_{VV0,max}$
 $\rightarrow VVm\pm 0$, inverted switching order,
 $h_{VV0}=h_{VV0,min}$

For branch A $\rightarrow G$, $h_{VV0,min}$ is set to

$$h_{VV0,min} = \frac{\Delta\psi - \frac{1}{2} \cdot \Delta\psi_{ZV}}{|\dot{\psi}_{s,VV0}|} \quad (18a)$$

whereas for branch F $\rightarrow G$:

$$h_{VV0,min} = C_4 \cdot \frac{\Delta\psi - (t_s - h_{VV1}) \cdot \dot{\psi}_{s,ZV}}{\dot{\psi}_{s,VV0}} \quad (18b)$$

Since branch condition A (fig. 5) checks for a somewhat critical flux decrease, Eq. 18a results in longer on-times. Setting $C_4 = \frac{1}{2}$, Eq. 18b assumes that, in the succeeding cycle, $VVm\pm 1$ will provide a certain flux increase, too.

Some additional constraints are generally included for the branch conditions to avoid suspicious switching patterns:

- When entering „Force Flux-Supporting VV“ mode, a flag is set. After this cycle, we never use flux decreasing $VVm\pm 2$.
- „Force Flux-Supporting VV“ mode is never entered after a cycle with $VVm\pm 2$.

In the following section some simulations will illustrate the smooth behaviour of these to some extent complex rules.

SIMULATION RESULTS

The algorithm has been checked out first with some simulations. To analyse the inner torque control loop without further influences we propose a brief start-up with constant torque (i. e. 50% of rated torque T_{rated}), followed by a deceleration of about 10% T_{rated} . Since we want primarily illustrate the working principle of the torque controller, the simulation uses ideal parameters. Furthermore, it neglects the delay of the inner prediction model that would in reality be caused by the computation time. Fig. 6 shows an example.

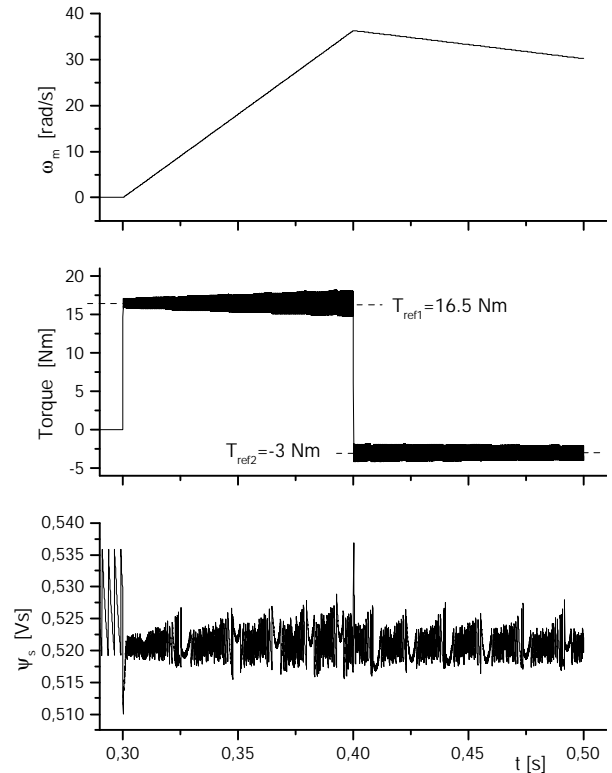


Figure 6: Simulation of improved DMTC, $T_{ref} = const.$

At the beginning, $T_{ref} = 0$ yet, only „Force Flux-Supporting VV“ mode intervenes to apply VVs. During acceleration, the „virtual hysteresis“ enlarges due to increasing $|\dot{T}_{ZV}|$. Requesting lower torque at

lower angular speed leads to short on-times h_{VV} which yields to significant interference of the flux controller. Some alterations of the flux phasor may be observed, whereas torque outliers do not appear.

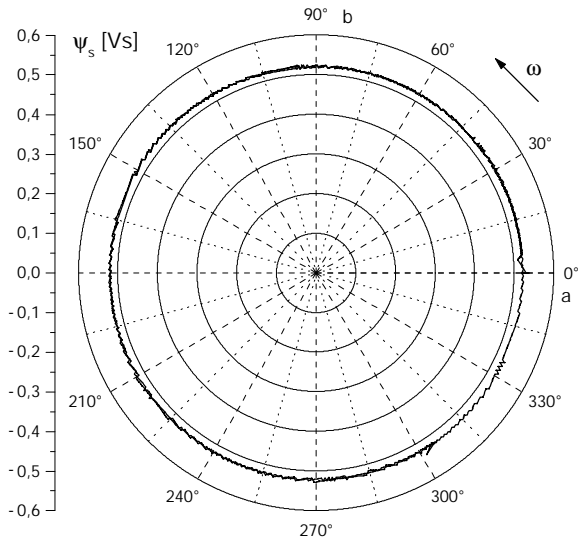


Figure 7: Trajectory of flux phasor (cf. fig. 6)

The polar diagram of the flux phasor (fig. 7) proves, that even the flux alterations are not very important. Fig. 8 presents a more detailed view of the controller's behaviour. In this extract, the controller mostly enters "Normal mode". Due to the fact that, just before

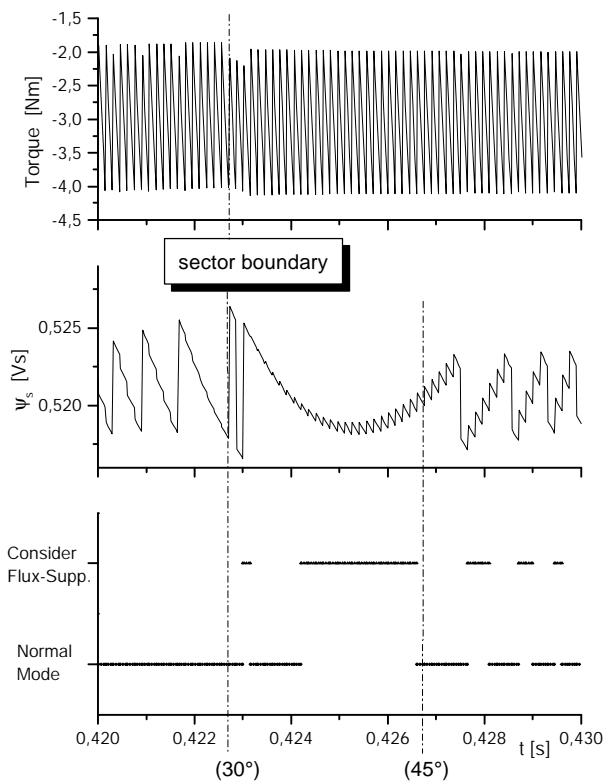


Figure 8: Details of controller behaviour (cf. fig. 6)

passing the sector boundary, the $VV_{m\pm 2}$ decreases the flux only little, some switching of $VV_{m\pm 1}$ is sufficient to refresh the flux. After passing the sector boundary, "Consider Flux-Supporting VV" leads to a few $VV_{m\pm 0}$. Due to $\dot{T}_{VV0} < \dot{T}_{VV1}$, the "virtual hysteresis" and its offset slightly vary.

EXPERIMENTAL RESULTS

The whole control scheme has been implemented on a signal processor TMS320C30 at 40 MHz, mainly in highlevel programming language C. The cycle time was set to $150\mu s$, leading to a switching frequency of 3.33 kHz per transistor. This time includes data acquisition, a speed controller, and some extensions for experimental purposes and as well. The following fig. 9 depicts an oscilloscope screenshot of the program test.

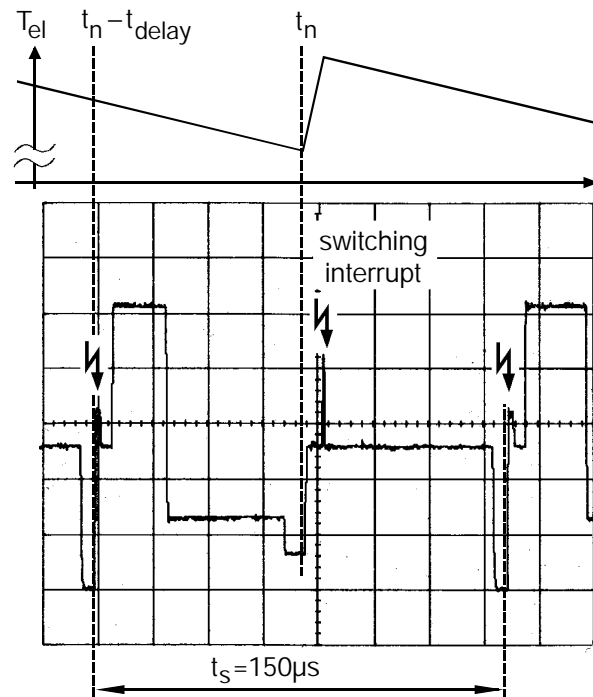


Figure 9: Oscilloscope screenshot of program test

At the beginning of the interrupt routine we intend to reserve some time for position and speed control. After estimating the new torque reference T_{ref} , the preselection of the $VV_{m\pm 0,1,2}$ is done, followed by the torque and flux control algorithms. In order to synchronize accurately to real-time, the delay until switching the VV has been fixed to $t_{delay} = 70\mu s$. In this experimental set-up, the second timer of the DSP is employed to generate a switching interrupt. The prediction of the model is performed in two steps (h_{VV} , h_{ZV}) after

switching the VV. Fig. 10 shows an experiment similar to the simulation in fig. 6.

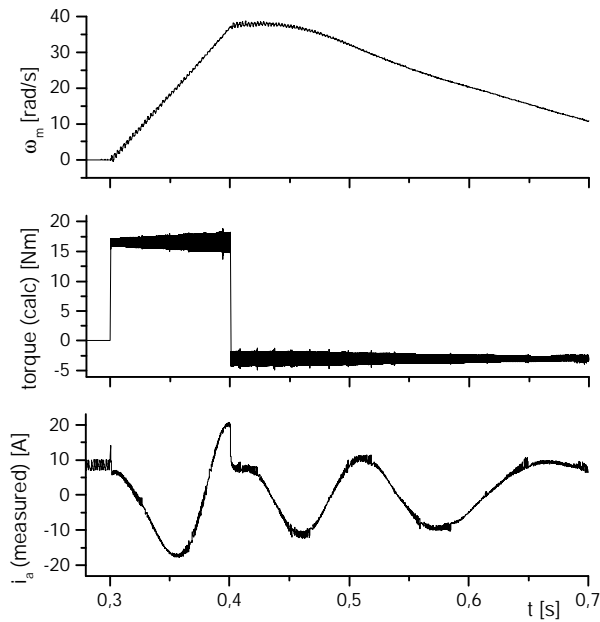


Figure 10: Experimental start-up, $T_{ref1} = 16.5$, $T_{ref2} = -3$

The start-up with constant torque works well. A fast change of the measured phase current can also be noticed. Due to the poor open loop observer without current feedback, the deceleration is not as uniform as in the simulation. Finally, fig. 11 focuses on a special problem of the experimental set-up. As a result of the extremely short torque rise time, a strong mechanical resonance can be observed.

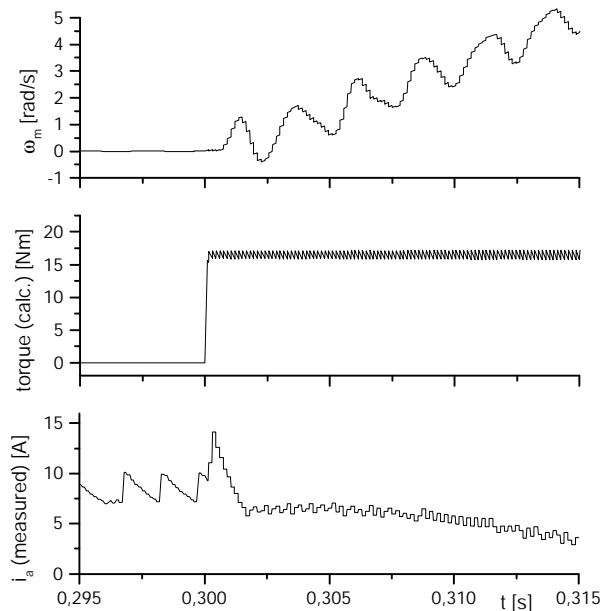


Figure 11: Mechanical oscillations of experim. set-up

CONCLUSION

A novel algorithm for DMTC is proposed. A new equation for the on-time of the VV and the ZV provides to reach steady state directly at the end of a fixed cycle. The predictive algorithm calculates two switching states in advance. Thus, it is possible to switch a VV for a very short time. This allows to exploit machines with extremely small leakage inductance. The currents can be changed very fast, and the torque as well, resulting in very high dynamic performance.

The algorithm seems to be rather complicate to realize. In conclusion, this is not the case. Many of the rules proposed for the flux controller have implicit relations. Observer and speed controller are still a subject of our research.

REFERENCES

- [1] Takahashi, I., Noguchi, T.: A New Quick-Response and High-Efficiency Control Strategy of an Induction Motor“, IEEE Transactions of Industry Applications, Vol. IA-22, No. 5, Sept./Oct. 1986)
- [2] Depenbrock, M.: Direkte Selbstregelung (DSR) für hochdynamische Drehfeldantriebe mit Stromrichterspeisung, etzArchiv, Bd. 7, 1985, Heft 7, S. 211-218
- [3] Aaltonen, M., Tiitinen, P., Lalu, J., Heikkilä S.: Direkte Drehmomentregelung von Drehstromantrieben, ABB Technik 3/1995, S. 19-24
- [4] Stadtfeld, S.: Das Verfahren zur Regelung der pulsumrichtergespeisten Asynchronmaschine durch Prädiktion und Optimierung in Echtzeit Dissertation Wuppertal 1987
- [5] Lochot, Ch., Roboam, X., Maussion, P.: A New Direct Torque Control Strategy for an Induction Motor with Constant Switching Frequency Operation, EPE Sevilla/Spain 1995, Vol.2, S. 431-436
- [6] Flach, E., Hoffmann, R., Mutschler, P.: Direct Mean Torque Control of an Induction Motor, EPE Trondheim/Norwegen 1997, Vol. 3, S. 672-677

PARAMETERS

$R_1 = 0.79 \ \Omega$	$L_1 = 66.57 \ \text{mH}$
$R_2 = 0.76 \ \Omega$	$L_2 = 66.59 \ \text{mH}$
$L_h = 65. \ \text{mH}$	$\Psi_{ref} = 0.52 \ \text{Vs}$
$n_N = 1500 \ \text{min}^{-1}$	$T_{rated} = 33 \ \text{Nm}$
$Z_p = 2$	$U_{dc} = 540 \ \text{V}$
	$f_N = 50 \ \text{Hz}$